Lactosylceramide: Lateral Interactions with Cholesterol

Xiuhong Zhai, Xin-Min Li, Maureen M. Momsen, Howard L. Brockman, and Rhoderick E. Brown
University of Minnesota, Hormel Institute, Austin, Minnesota

ABSTRACT Lactosylceramide (LacCer) is a key intermediate in glycosphingolipid metabolism and is highly enriched in detergent-resistant biomembrane fractions associated with microdomains, i.e., rafts and caveolae. Here, the lateral interactions of cholesterol with LacCers containing various homogeneous saturated (8:0, 16:0, 18:0, 24:0) or monounsaturated acyl chains (18:1, 24:1) have been characterized using a Langmuir-type film balance. Cholesterol-induced changes in lateral packing were assessed by measuring changes in average molecular area, i.e., area condensations, and in lateral elasticity, i.e., surface compressional moduli (C_S^{-1}) with emphasis on high surface pressures ($\geq$30 mN/m) that mimic biomembrane conditions. Cholesterol most dramatically affected the lateral packing elasticity of LacCers with long saturated acyl chains at sterol mole fractions $\geq$0.3, consistent with liquid-ordered (LO) phase formation. The lateral elasticity within the LacCer-cholesterol LO-phase was much lower than that observed within pure LacCer condensed, i.e., gel, phase. The magnitude of the cholesterol-induced reduction in lateral elasticity was strongly mitigated by *cis* monounsaturation in the LacCer acyl chain. At identical high sterol mole fractions, higher lateral elasticity was observed within LacCer-cholesterol mixtures compared with galactosylceramide-cholesterol and sphingomyelin-cholesterol mixtures. The results show how changes to sphingolipid headgroup and acyl chain structure contribute to the modulation of lateral packing elasticity in sphingolipid-cholesterol LO-phases.

INTRODUCTION

Heterogeneity in the lateral organization of lipids in biomembranes has been contemplated for many years (1) eventually leading to current microdomain models. In the raft/caveolar model, microdomains enriched in sphingolipids and cholesterol putatively function as targeted surface interaction sites by acting as organizing platforms that attract proteins with certain types of lipid anchors (2–4). Although there is general agreement regarding the existence of lateral confinement domains in cell membranes, controversy persists as to whether the decreased lateral diffusion can be attributed to lipid rafts or to proteins acting as fences (5–10). In model membranes, domains can be observed in the absence of proteins at certain lipid mixing ratios of sphingomyelin (SM), phosphatidylcholine (PC), and sufficiently high cholesterol (11–14). At high cholesterol mole fractions (>0.3), the resulting lipid phase is often described as liquid-ordered (LO) to emphasize the liquid-like lateral mobility and highly ordered nature of the hydrocarbon chains (15–19). It has been suggested that cholesterol-induced changes in membrane thickness and fluidity are critical features responsible for modulation of the lateral distributions of certain integral membrane proteins (20), of peripheral membrane proteins with certain lipid anchors (21,22), and of glycosphingolipids (GSLs), i.e., lactosylceramide and ganglioside GM1 (11,23). Exactly how changes in membrane thickness and fluidity in LO phase manifest themselves physically to drive the lateral reorganization of certain membrane proteins and lipids has remained somewhat elusive. Recently, new insights into LO phase physical characteristics have emerged. Theoretical calculations and experimental data in monolayers and bilayers have revealed that the dramatically lower lateral elasticity of the cholesterol-induced LO phase is likely to be a major potentiator of changes in the lateral distribution of integral proteins and of glycosphingolipids in membranes and of lipid resistance to solubilization by detergents (24–30).

Among membrane lipids, sphingolipids are particularly well-suited for formation of LO phase because of their ability to donate and accept hydrogen bonds during intermolecular encounters and their naturally high preponderance of saturated acyl chains. Lactosylceramides (LacCer) are sphingolipids, with uncharged disaccharide headgroups, that are highly enriched in the caveolar and detergent-resistant fractions of cell isolates (21,23) and that modulate the integrin-driven formation of cellular microdomains (31). Alteration in the levels and distribution of cholesterol in certain sphingolipid storage diseases, i.e., Niemann-Pick type C, is responsible for the aberrant targeting of internalized LacCer to the lysosomes instead of the Golgi compartment (32). LacCer is also a pivotal intermediate in the metabolism of many complex GSLs including gangliosides (i.e., GM3, ABO blood-type) and has been implicated in cell-cell and cell-matrix interactions and in signaling events linked to cell differentiation, development, apoptosis, and oncogenesis (33–35). Because of the important cellular processes involving LacCer, gaining insights into how this sphingolipid interacts with other membrane lipids is of timely importance.

Currently, information about the lateral interactions of LacCer with cholesterol in model and biological membranes

Submitted March 10, 2006, and accepted for publication June 14, 2006.

Xiuhong Zhai and Xin-Min Li contributed equally to this work.

Address reprint requests to Rhoderick E. Brown, E-mail: rebrown@hi.umn.edu or reb@umn.edu.

Xin-Min Li's present address is Dept. of Cell Biology, Lerner Research Institute, Cleveland Clinic, Cleveland, Ohio.

0006-3495/06/10/2490/11 $2.00

doi: 10.1529/biophysj.106.084921

is nearly nonexistent. In this study, we synthesized different physiologically relevant LacCer species to facilitate clear-cut analysis of their mixing behavior with cholesterol and used Langmuir film balance approaches to analyze changes in the average cross-sectional area behavior and changes in resistance to lateral compression/extension, i.e., lateral elasticity. The results, obtained with a half dozen different LacCer species (Fig. 1) mixed with cholesterol mole fractions covering the typical range observed in biomembranes, are discussed within a framework of previous findings involving sterol interactions with SMs and galactosylceramides (GalCer).

EXPERIMENTAL PROCEDURES

Cholesterol was obtained from NuChek Prep (Elysian, MN). Different LacCer species with homogeneous acyl chains were produced by reacylating D-lactosyl-β1-1′-D-erythro-sphingosine (lyso LacCer; Avanti Polar Lipids, Alabaster, AL) with the desired fatty acyl chain as described previously (36). Briefly, the *N*-hydroxy succinimide esters of different fatty acids were prepared, recrystallized, and reacted with lyso-LacCer. Reacylation was performed at 60°C under nitrogen for 6–8 h in the presence of the catalyst, *N*-ethyldiisopropylamine. After reacylation, LacCer was purified by flash column chromatography and crystallized from $CHCl_3/CH_3OH$ using −20°C acetone. The approach enabled preparation of *N*-hexadecanoyl lactosylsphingosine (16:0 LacCer), *N*-octadecanoyl lactosylsphingosine (18:0 LacCer), *N*-tetracosanoate lactosylsphingosine (24:0 LacCer), *N-cis*-9-octadecenoate lactosylsphingosine, (18:1 LacCer), *N-cis*-15-tetracosenoate lactosylsphingosine (24:1 LacCer). *N*-octanoyl lactosylsphingosine (8:0 LacCer) was obtained from Avanti Polar Lipids. LacCer purity and *N*-acyl homogeneity were confirmed to be >99% by TLC and by capillary gas chromatography, respectively. Final stock concentrations were determined by dry weight using a Cahn microbalance (model 4700).

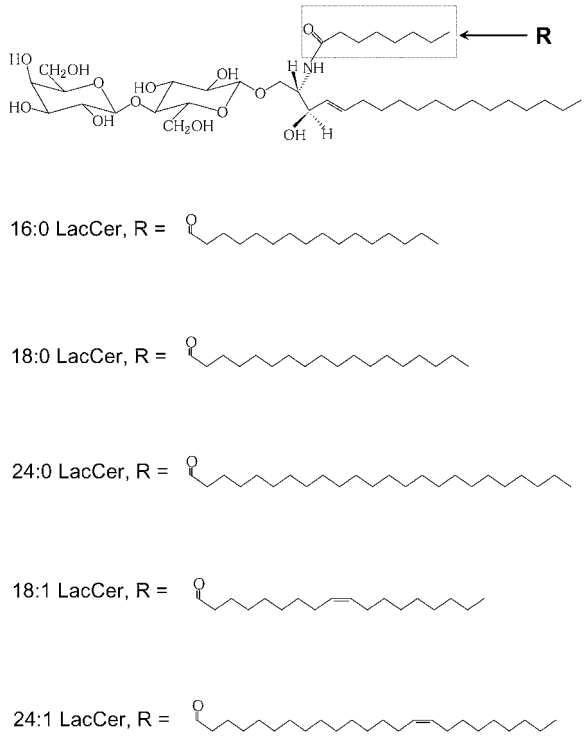

FIGURE 1 Structure of LacCer Species. The LacCer depicted is 8:0 LacCer. Other LacCer species were synthesized using the various fatty acyl residues (*R* groups) and purified as described in the Experimental Procedures. The conformational arrangement is based on NMR data (72).

Monolayer conditions

Surface pressure-molecular area (π-A) isotherms were measured using a computer-controlled, Langmuir-type film balance, calibrated according to the equilibrium spreading pressures of known lipid standards (38). Lipids were mixed and spread (51.67 μl aliquots) from stock solutions dissolved in toluene/ethanol (5:6) or hexane/isopropanol/water (70:30:2.5). Solvent purity was verified by dipole potential measurements using a ^{210}Po ionizing electrode (39). After spreading on the subphase surface, lipid films were compressed at a rate of $\leq$4 Å^2/molecule/min after a delay period of 4 min. Subphase buffer was maintained at 24°C via a thermostated, circulating water bath and was produced using water that had been purified by reverse osmosis, activated charcoal adsorption, mixed-bed deionization, then passed through a Milli-Q UV Plus System (Millipore, Bedford, MA), and filtered through a 0.22 μm Millipak 40 membrane. Subphase buffer contained 10 mM potassium phosphate (pH 6.6), 100 mM NaCl, and 0.2% NaN_3 and was kept stored under argon, which was cleaned by passage through a seven-stage series filtration set-up consisting of an Alltech activated charcoal gas purifier, a LabClean filter, and a series of Balston disposable filters consisting of two adsorption (carbon) and three filter units (93% and 99.99% efficiency at 0.1 μm). The film balance was separately enclosed under humidified argon and was housed in an isolated laboratory supplied with clean air by a Bioclean Air Filtration system equipped with charcoal and HEPA filters. Other features contributing to isotherm reproducibility include automated lipid spreading via a modified HPLC autoinjector, automated surface cleaning by multiple barrier sweeps between runs, and highly accurate and reproducible setting of the subphase level by an automated aspirator. Glassware was acid cleaned, rinsed with purified water, and then with hexane/ethanol (95:5) before use.

To keep with recent proposals (40) we avoid using the term ''liquid condensed'' and instead use the term ''condensed'' to denote the monolayer state in which the hydrocarbon chains are ordered. The condensed state contrasts the liquid-expanded state in which the chains are conformationally disordered. Monolayer data were analyzed using Film Fit (Creative Tension, Austin, MN). Monolayer phase transitions between the liquid-expanded and condensed states were identified from the second and third derivatives of surface pressure (π) with respect to molecular area (*A*) (41,42). Monolayer compressibilities at the indicated experimental mixing ratios were obtained from π-A data using

$$C_s = -\frac{1}{A}\left(\frac{\partial A}{\partial \pi}\right)_T, \quad (1)$$

where *A* is the area per molecule at the indicated surface pressure (π). To facilitate comparison with elastic moduli of area compressibility values in bilayer systems (24,42–45), we expressed our data as the reciprocal of C_S, originally defined as the surface compressional modulus (C_S^{-1}) by Davies and Rideal (45). Whenever possible, we used a 100-point sliding window that utilized every fourth point to calculate a C_S^{-1} value before advancing the window one point. Reducing the window size by fivefold did not significantly affect the observed C_S^{-1} values. Each plot of C_S^{-1} versus average molecular area consisted of 200 C_S^{-1} values obtained at equally spaced molecular areas along the π-A isotherms. High C_S^{-1} values correspond to low lateral elasticity among packed lipids forming the monolayer. The standard errors of the C_S^{-1} values are ~2%. We found pure cholesterol monolayers, which are highly condensed, to have C_S^{-1} values of 1126, 1551, and 1540 mN/m at 10, 20, and 30 mN/m, respectively, in agreement with Merkel and Sackmann (46). We have previously characterized the C_S^{-1} values of different LacCer species in pure form at different temperatures (36). Comprehensive descriptions of the mechanoelastic properties of model membranes have been reviewed by Needham (47) and Behroozi (48).

Analyses of LacCer and cholesterol mixtures

The area condensing effect of cholesterol on different LacCer species was determined from plots of average molecular area versus composition (25,49). Experimentally observed areas of mixtures were compared with areas calculated by summing the molecular areas of the pure components (apportioned by mole fraction in the mixture). The calculated average molecular area (A) of two component mixtures was determined at a given surface pressure (π) using the following equation:

$$A = X_1(A_1) + (1 - X_1)(A_2), \quad (2)$$

where X_1 is the mole fraction of component 1, and A_1 and A_2 are the molecular areas of pure components 1 and 2 at identical surface pressures. Negative deviations from additivity indicate area condensation and imply intermolecular accommodation and/or dehydration interactions between the lipids in the mixed films.

To complement the area condensation data, monolayer compressibilities (C_S) were obtained from π-A data at the indicated experimental mixing ratios using Eq. 1 (described above). Ideal mixing was modeled by apportioning the C_S value for each lipid (as a pure entity) by both molecular area fraction and mol fraction as described previously (49–51). Thus, at a given constant surface pressure (π),

$$C_s = (1/A)((C_{s1}A_1)X_1 + (C_{s2}A_2)X_2), \quad (3)$$

where $X_2 = (1 - X_1)$ and C_S is additive with respect to the product ($C_{Si}A_i$) rather than (C_{Si}) for either ideal or completely nonideal mixing. Deviations of experimental values from calculated ideality indicate that the lipid components of the mixed monolayers are partially nonideally mixed. Data were expressed in terms of the surface compressional modulus (C_S^{-1}), to facilitate comparisons with elastic moduli of area compressibility determinations in bilayer systems. We have previously characterized the response of C_S^{-1} to changes in LacCer acyl structure and phase state, as well as mixing interactions of cholesterol with various PC and SM species (49–51). The C_S^{-1} values of PC-cholesterol and SM-cholesterol mixed monolayers are strongly affected by PC and SM acyl structure. When mixed with equivalent high cholesterol mole fractions, PCs and SMs with saturated acyl chains have much higher C_S^{-1} values (lower lateral elasticity) than PCs (and SMs) with unsaturated acyl chains suggesting that *cis* double bonds can act as interfacial ''springs'' that mitigate the capacity of cholesterol to reduce lateral elasticity. C_S^{-1} analyses utilize data available in the slopes of the isotherms and are especially informative for providing insights into the effects of cholesterol at high surface pressures thought to mimic the biomembrane environment (52,53). Thus, C_S^{-1} measurements complement area condensation data which are inherently less reliable at high surface pressures because of the associated small changes in average area.

RESULTS

LacCer species with palmitoyl (16:0), stearoyl (18:0), and lignoceroyl (24:0) acyl Chains

Our initial goal was to characterize the interaction of cholesterol with LacCers containing different, physiologically-relevant, saturated acyl chains while focusing on the cholesterol mole fraction range directly relevant to biological membranes (0–0.6 mol fractions). The investigative strategy relied on synthesis and purification of LacCer species containing uniform-length, 18-carbon sphingosine base chains and select N-acyl chains of differing lengths (Fig. 1). Fig. 2, *A–C*, shows the π-A isotherms for cholesterol mixed with 16:0 LacCer, 18:0 LacCer, and 24:0 LacCer. At 24°C, each of the pure LacCer species show condensed phase behavior with no obvious phase transitions and relatively small collapse areas (<42 Å^2 per molecule), suggesting that their disaccharide polar headgroups project from the interface in a more perpendicular than parallel fashion and that their hydrocarbon chains are highly ordered (36,37). Pure cholesterol is known to form solid condensed monolayers and behaves as a small, relatively ''fixed-area'' lipid (36–38 Å^2 per molecule) (25,27,46). Thus, as the cholesterol mole fraction increases, small decreases are expected in the average molecular cross-sectional areas of the lipid mixtures. At surface pressures <20 mN/m, stepwise increases in the sterol content of 16:0 LacCer-cholesterol mixtures did produce the anticipated incremental decreases in the average molecular areas within the isotherms (Fig. 2 *A*). However, at surface pressures above 20–25 mN/m, the expected decrease in average molecular area was nonexistent for 16:0 LacCer-cholesterol (Fig. 2 *A*), and was limited to cholesterol mole fractions of 0.1 or 0.2 for 18:0 LacCer and for 24:0 LacCer (Fig. 2, *B* and *C*). Rather,

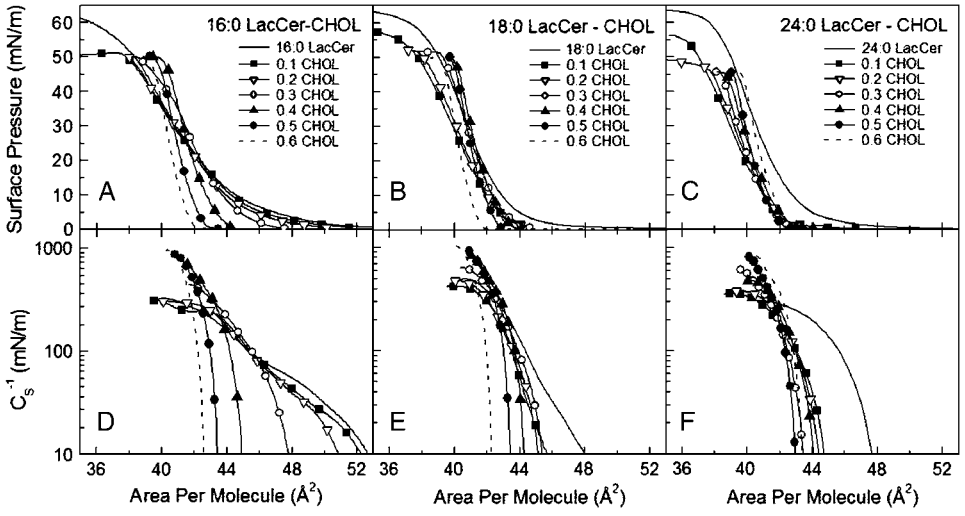

FIGURE 2 Effect of cholesterol on 16:0 LacCer, 18:0 LacCer, and 24:0 LacCer interfacial behavior. The surface pressure versus average cross-sectional molecular area (π-A) isotherms and the surface compressional modulus versus average cross-sectional molecular area (Cs^{-1}-A) responses are shown for 16:0 LacCer/cholesterol (*A* and *D*), 18:0 LacCer/cholesterol (*B* and *E*), and 24:0 LacCer/cholesterol (*C* and *F*), respectively. Data were collected at 24°C. Isotherms (from *right* to *left* at 5 mN/m) contain 0, 0.1, 0.2, 0.3, 0.4, 0.5, and 0.6 mol fraction of cholesterol. Matching line styles in the upper and lower panels indicate equivalent cholesterol content.

incrementally increasing area expansions were observed with further stepwise increases in cholesterol mole fraction at surface pressures > 25 mN/m.

To determine whether ordering/disordering of the LacCer hydrocarbon chains by cholesterol contributed to the observed changes in average molecular area, the mixtures were analyzed using classic average molecular area versus composition plots (Fig. 3, *A–C*). Straight lines represent ideal additivity calculated from the cross-sectional molecular areas of pure cholesterol and each LacCer species and apportioned by mole fraction at three different surface pressures (5, 15, and 30 mN/m). 16:0 LacCer-cholesterol mixtures showed no evidence of cholesterol-induced area condensation, i.e., negative deviation from ideal additivity, at either low or high pressure (Fig. 3 *A*). Rather, a small positive deviation from ideal additivity was observed at high pressure. In 18:0 LacCer-cholesterol and 24:0 LacCer-cholesterol mixtures, small ''condensing effects'' were produced by 0.1 mol fraction cholesterol. The ''condensing effect'' was observed only at low pressure (5 mN/m) for monolayers containing 18:0 LacCer, but was evident at all surface pressures, including 30 mN/m, for monolayers containing 24:0 LacCer. The area condensations diminished with increasing cholesterol content. Positive deviations from ideal additivity, i.e., expansion effect, were observed at sterol mole fractions of 0.4 and higher.

Because the absolute area changes associated with the deviations from ideal additivity were small, analyses were performed to take advantage of additional information contained in the isotherms. Evaluations of isotherm shape, obtained from their surface compressional moduli, C_S^{-1}, provide insights into changes in the lateral packing elasticity induced by temperature or by mixing with other lipids (24,41,42, 45,49–51). Fig. 2, *D–F*, show the C_S^{-1} versus average molecular area behavior for the LacCer-cholesterol mixtures at different sterol mole fractions. At higher surface pressures ($\pi > 20$ mN/m), the C_S^{-1} versus average molecular area plots for 16:0 LacCer-cholesterol mixtures formed two groups, delineated by dramatically different slopes and depending on whether the cholesterol mole fraction was greater or less than ~0.3 (Fig. 2 *D*). For 18:0 LacCer-cholesterol and 24:0 LacCer-cholesterol monolayers, the C_S^{-1} versus average molecular area behavior was somewhat less clear with respect to the two groups delineated by cholesterol mole fractions greater or less than ~0.3.

C_S^{-1} versus composition plots were constructed to further evaluate the mixtures (Fig. 4, *A–C*). Lines without symbols represent theoretical ideal mixing calculated from the C_S^{-1} values of 16:0 LacCer, 18:0 LacCer, 24:0 LacCer and of pure cholesterol, apportioned by both mole and area fraction. Because of this apportioning, the theoretical ideal mixing lines are curvilinear, with increasing C_S^{-1} values indicating decreasing lateral elasticity (49–51). Fig. 4, *A–C* (*triangles*) shows the results obtained at 30 mN/m, which was of interest because high monolayer surface pressures mimic the packing environment of biological membranes (e.g., 52). It is noteworthy that cholesterol mole fractions up to 0.2 have relatively modest effects on the C_S^{-1} values of all three LacCer species regardless of the severity of their intramolecular chain length asymmetry. Above 0.2 mol fraction, the C_S^{-1} values increased more rapidly and were accompanied by large deviations from ideal additivity. This biphasic response in the C_S^{-1} values was consistent with the onset of cholesterol-induced, liquid-ordered phase. With 24:0 LacCer-cholesterol mixtures, a more uniform upward curvature of C_S^{-1} values was observed as the cholesterol content increased. The steady increases in C_S^{-1} values as a function of increasing cholesterol indicated decreasing lateral elasticity. The net result was a ~2.5-fold decrease in the lateral packing elasticity for all three LacCer species with long saturated acyl chains when mixed with equimolar cholesterol compared to their pure glycolipid states regardless of intramolecular chain-length asymmetry.

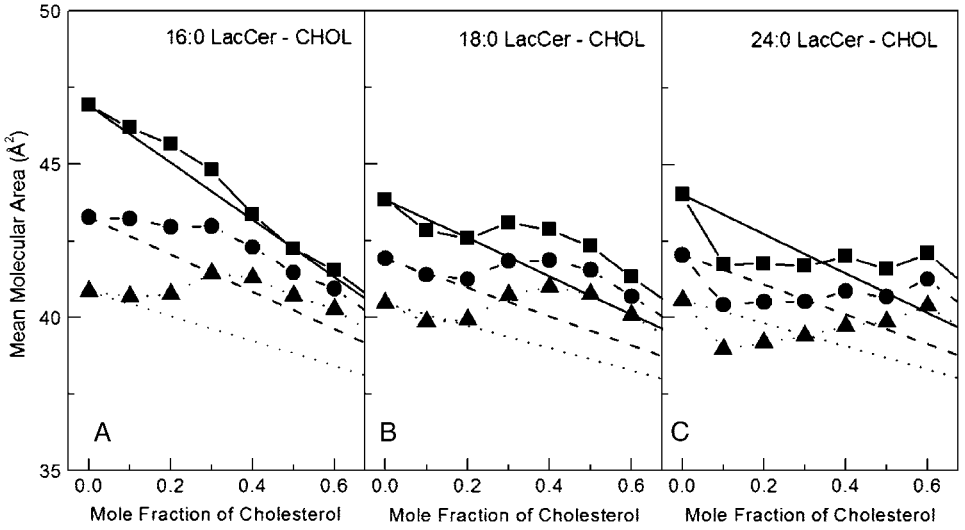

FIGURE 3 Average molecular area versus composition analyses. (*A*) 16:0 LacCer/cholesterol, (*B*) 18:0 LacCer/cholesterol, and (*C*) 24:0 LacCer/cholesterol. Data are shown at 5 (■), 15 (●), and 30 (▲) mN/m. Lines with symbols represent the experimental response. The straight lines without symbols represent the theoretical additive behavior calculated from the response of the pure lipids as described in the Experimental Procedures. Because the theoretical binary mixtures are apportioned by mole fraction, the responses are linear.

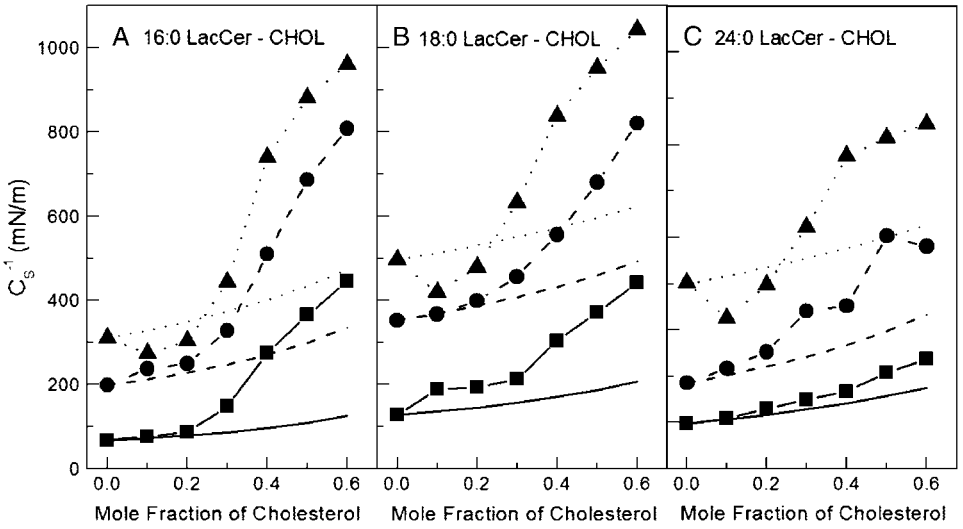

FIGURE 4 Average surface compressional modulus versus composition analyses. (*A*) 16:0 LacCer/cholesterol, (*B*) 18:0 LacCer/cholesterol, and (*C*) 24:0 LacCer/cholesterol. Data are shown at 5 (■), 15 (●), and 30 (▲) mN/m. Lines with symbols represent the experimental data. Lines without symbols represent the theoretical additive behavior calculated from the response of the pure lipids as described in the Experimental Procedures. Because the theoretical binary mixtures are apportioned by both mole and area fraction, the responses are nonlinear.

LacCer species with octanoyl (8:0), oleoyl (18:1), and nervonoyl (24:1) acyl chains

Although the studies with 16:0, 18:0, and 24:0 LacCer enabled characterization of the interaction of cholesterol with LacCers containing long, saturated acyl chains, the three LacCer species all exhibited high major enthalpic phase transition temperatures that result in condensed phase behavior at physiologic temperature (36). It was also of interest to investigate how fluid-phase LacCers interact with cholesterol. Structural changes included shortening of the saturated acyl chain (e.g., 8:0) and introduction of *cis* unsaturation into saturated acyl chains of differing length (e.g., $18{:}1^{\Delta 9cis}$ and $24{:}1^{\Delta 15cis}$). As shown in Fig. 5, *A* and *B*, LacCer containing either octanoyl (8:0) or oleoyl ($18{:}1^{\Delta 9cis}$) acyl chains both displayed fluid, chain-disordered, liquid-expanded behavior in pure form; whereas the isotherms of LacCer with nervonoyl ($24{:}1^{\Delta 15cis}$) acyl chains (Fig. 5 *C*) showed clear evidence of a metastable phase transition with an onset pressure near 20 mN/m at 24°C. The relatively large areas per molecule observed in the absence of sterol were consistent with the short saturated and long *cis*-unsaturated acyl chains having significant disordering effects on LacCer lateral packing. Increasing the cholesterol content of mixed monolayers containing the LacCer species resulted in substantial reductions in the average area per molecule (Fig. 5, *A–C*). Although decreases in average molecular area were expected with increasing sterol content because cholesterol occupies substantially smaller cross-sectional area than liquid-expanded LacCers, the extent to which ordering of the LacCer hydrocarbon chains by cholesterol also contributed to the observed decreases in average molecular area was not clear. To address this issue, the mixtures were analyzed using classic average molecular area versus composition plots (Fig. 6, *A–C*). Straight lines represent ideal additivity calculated from

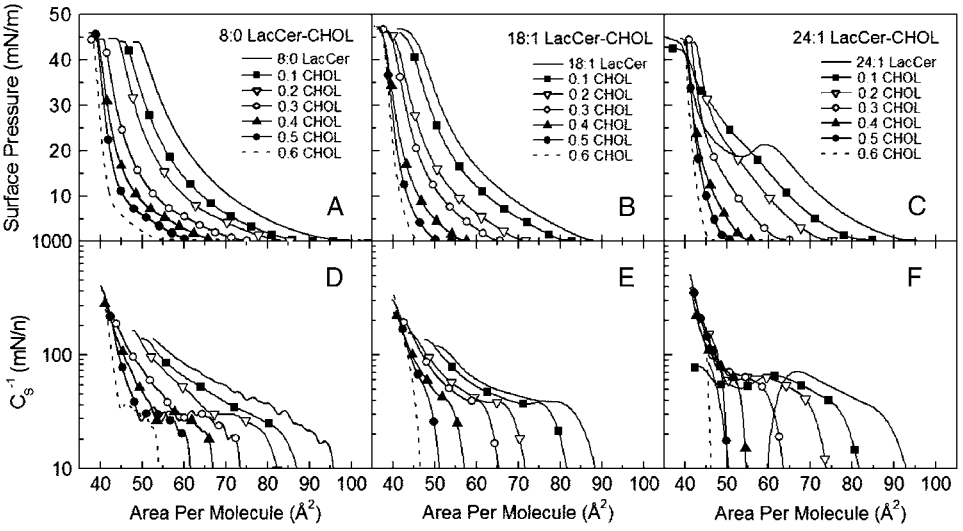

FIGURE 5 Effect of cholesterol on 8:0 LacCer, 18:1 LacCer, and 24:1 LacCer interfacial behavior. The surface pressure versus average cross-sectional molecular area (π-A) isotherms and the surface compressional modulus versus average cross-sectional molecular area (Cs^{-1}-A) responses are shown for 8:0 LacCer/cholesterol (*A* and *D*), 18:1 LacCer/cholesterol (*B* and *E*), and 24:1 LacCer/-cholesterol (*C* and *F*), respectively. Data were collected at 24°C. Isotherms (from *right* to *left* at 5 mN/m) contain 0, 0.1, 0.2, 0.3, 0.4, 0.5, and 0.6 mol fraction of cholesterol. Matching line styles in the upper and lower panels indicate equivalent cholesterol content.

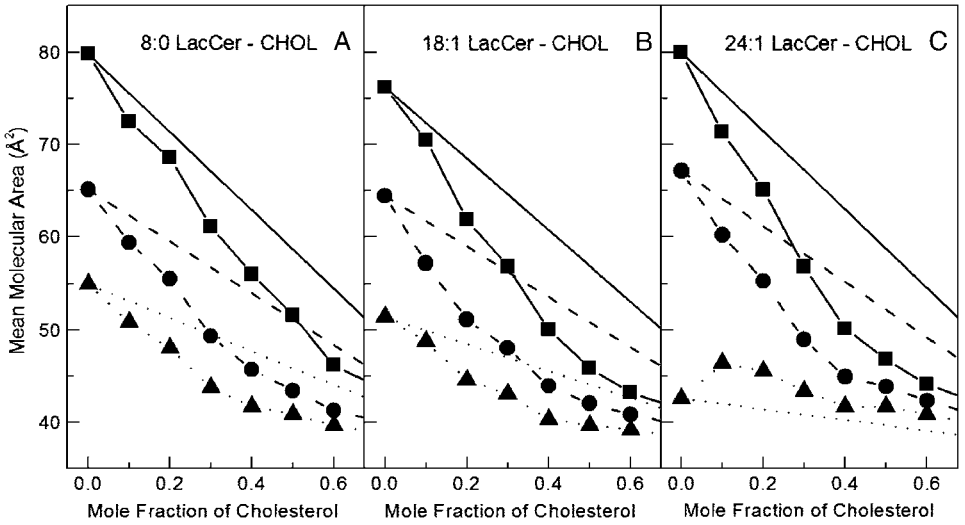

FIGURE 6 Average molecular area versus composition analyses. (*A*) 8:0 LacCer/cholesterol, (*B*) 18:1 LacCer/cholesterol, and (*C*) 24:1 LacCer/cholesterol. Data are shown at 5 (■), 15 (●), and 30 (▲) mN/m. Lines with symbols represent the experimental response. The straight lines without symbols represent the theoretical additive behavior calculated from the response of the pure lipids as described in the Experimental Procedures. Because the theoretical binary mixtures are apportioned by mole fraction, the responses are linear.

the cross-sectional molecular areas of pure cholesterol and each LacCer species and apportioned by mole fraction at three surface pressures (5, 15, and 30 mN/m). Substantial negative deviations from additivity are evident at all surface pressures for both 8:0 LacCer and 18:1 LacCer. It is noteworthy that, for 24:1 LacCer-cholesterol mixtures, the negative deviations from additivity at 5 and 15 mN/m exceed the values observed for 8:0 LacCer and 18:1 LacCer mixed with equivalent amounts of cholesterol. However, at 30 mN/m, a surface pressure where 24:1 LacCer is no longer liquid-expanded, cholesterol has no ordering effect but rather moderately disrupts the glycolipid packing, as is shown by the positive deviation from ideal area additivity.

To gain additional insights into mixing behavior at surface pressures that mimic the lipid-cross sectional areas of biomembranes (e.g., 30 mN/m) the surface compressional moduli were analyzed as a function of cholesterol mole fraction. In contrast to monolayer area condensations, which provide maximal response at low surface pressures, the surface compressional moduli respond maximally at high surface pressures. Fig. 7 shows the C_S^{-1} versus composition plots for 8:0 LacCer, 18:1 LacCer, and 24:1 LacCer over the cholesterol mole fraction of 0–0.6. Lines without symbols represent theoretical ideal mixing calculated for each LacCer species and cholesterol, apportioned by both mole and area fraction (49–51). It is noteworthy that the C_S^{-1} values in the absence of cholesterol at 30 mN/m are 124, 118, and 144 mN/m for 8:0, 18:1, and 24:1 LacCer, respectively, and reflect the chain disordered, liquid-expanded state of each LacCer species. Increasing levels of cholesterol had similar effects on the C_S^{-1} values of 8:0 LacCer and 18:1 LacCer in producing a smoothly increasing response. Compared to 18:0 LacCer mixed with equimolar cholesterol, the C_S^{-1} value attained by 18:1 LacCer was almost 65% lower, reflecting a substantially increased lateral packing elasticity. The overall response of 24:1 LacCer upon mixing with cholesterol differed from that

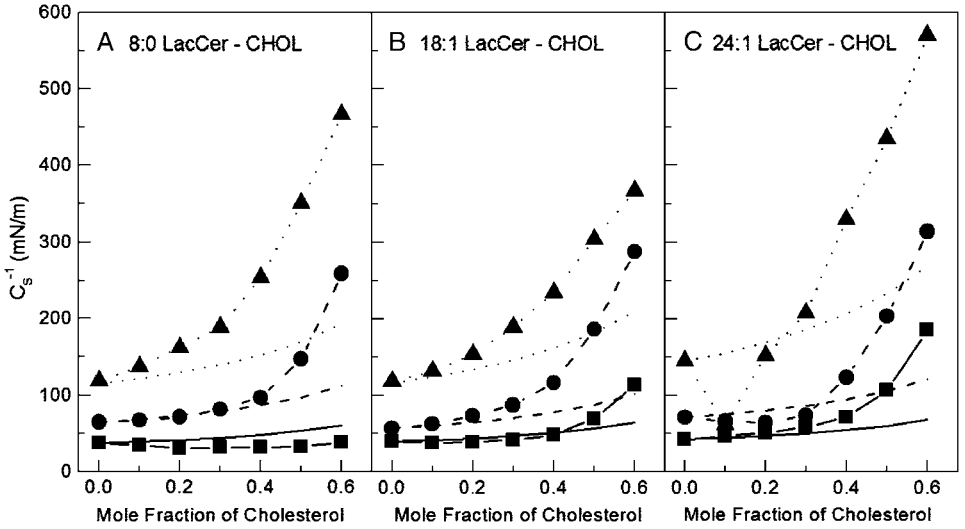

FIGURE 7 Average surface compressional modulus versus composition analyses. (*A*) 8:0 LacCer/cholesterol, (*B*) 18:1 LacCer/cholesterol, and (*C*) 24:1 LacCer/cholesterol. Data are shown at 5 (■), 15 (●), and 30 (▲) mN/m. Lines with symbols represent the experimental response. Lines without symbols represent the theoretical additive behavior calculated from the response of the pure lipids as described in the Experimental Procedures. Because the theoretical binary mixtures are apportioned by both mole and area fraction, the responses are nonlinear.

of 8:0 LacCer and 18:1 LacCer in that 24:1 LacCer showed a decrease in C_S^{-1} at 0.1 mol fraction cholesterol followed by a nearly linear increase between 0.1 and 0.6 mol fraction of cholesterol. Nonetheless, compared to 24:0 LacCer mixed with equimolar cholesterol, the C_S^{-1} value attained by 24:1 LacCer was almost 50% lower.

DISCUSSION

This study provides a comprehensive evaluation of the lateral interactions that occur between LacCer and cholesterol as well as insights into how physiologically relevant changes in LacCer structure modulate interactions with cholesterol. Gaining such insights is of timely importance because this GSL reportedly localizes to the cholesterol-enriched, detergent-resistant membrane fraction associated with rafts and caveolae (21,23) and has been associated with a number of key cellular processes. LacCer stimulates the expression of CD11/CD8, or Mac-1, on human neutrophil surfaces, thereby modulating a signal transduction pathway that triggers vascular endothelial cell proliferation, as mediated by TNF-α induced nuclear factor κB (NF-κB) and intercellular adhesion molecule (ICAM-1) (56). LacCer also is a receptor activator of NF-κB ligand and is essential for osteoclastogenesis as mediated by macrophage colony stimulation factor (57). Recently, LacCer has been shown to recruit PCKα/ε and phospholipase A_2 to stimulate PECAM-1 expression in human monocytes and adhesion to endothelial cells (58) and to regulate β1-integrin clustering and endocytosis on cell surfaces (31).

Lipid monolayers provide a model membrane system in which lipid lateral elasticity, i.e., ease/resistance to lateral compression, can be studied while maintaining the lipids in a uniform array that can be kept stable over a broad range of lipid compositions and phase states (e.g., 24,26,27,41,42,49,55). This experimental flexibility is not duplicated in bilayer model membranes where changes in lipid composition can manifest themselves as changes in the overall mesophasic organizational structure of the lipid aggregate, thus limiting the application of techniques such as micropipette aspiration that provides insights into bilayer lateral elasticity (*e.g.* 43,44,47). It is also noteworthy that lipid monolayers display most physical features associated with lipid bilayers (59), including the liquid-ordered phase, which was originally defined and modeled in monolayer lattices of cholesterol and DPPC (15) before extension to bilayers (16,17). For these reasons, lipid monolayer data can provide a resource to computational biophysicists who model lipid-lipid interactions and lipid lateral organization in membranes using powerful molecular dynamics and Monte Carlo simulation approaches (e.g., 60–63).

With the exception of a single model membrane study that examined an equimolar mixture of naturally-derived LacCer and cholesterol (64), information about the lateral interactions between LacCer and cholesterol has been almost nonexistent (54). The picture that emerges from our comprehensive study of interfacial interactions is the following: LacCers that display chain-disordered, liquid-expanded behavior show substantially larger cholesterol-induced reductions in average area compared to LacCers with ordered, condensed hydrocarbon chains. Moreover, cholesterol has a substantial ordering effect on the fluid-phase LacCers, even at cholesterol mole fractions of 0.1 or 0.2. The reductions in average area observed in LacCer-cholesterol mixtures dramatically exceed what is expected by simple replacement of LacCer with cholesterol, a molecule with a cross-sectional area that remains nearly unchanged in response to increasing surface pressure. Such area-condensing, chain-ordering effects are not observed in LacCers containing long saturated acyl chains, because the longer chains already exist in highly ordered states by virtue of enhanced van der Waals interactions that are manifested as higher thermotropic phase transition temperatures (36). The large ordering effect of high cholesterol mole fractions on LacCers containing short saturated or long monounsaturated acyl chains manifests itself as a substantial reduction in lateral elasticity (C_S^{-1} values go from ~120 to 300–350 mN/m; Table 1). Although this result is expected, what is remarkable is that high cholesterol levels also substantially reduce the lateral elasticity of LacCers with long saturated acyl chains that already exist in highly ordered states (e.g., relatively small cross-sectional areas) before mixing with cholesterol. As shown in Table 1, C_S^{-1} values ranged from 310 to 350 mN/m in the absence of cholesterol, consistent with the condensed, chain-ordered state of the LacCers. In the presence of equimolar cholesterol, the surface compressional moduli (C_S^{-1}) increased to 820–880 mN/m, values substantially higher than expected by replacement of LacCer with less compressible cholesterol (e.g., ideal additivity in Fig. 4). A plausible explanation for the preceding observations, based on the known features of the LO phase and condensed (gel) phases, is the following: Achievement of complete equilibrium for any condensed (gel) phase lipid, including long chain saturated LacCers (36), generally requires very long incubation (annealing) times at reduced temperatures and often exceeds 24 h. The nonequilibrium gel state can be expected to have occasional packing defects in the lattice structure of the monolayers. The packing defects persist because of the long range translational order and low translational mobility of lipids in the condensed (gel) phase. The presence of packing defects in the lattice creates voids that can increase lateral compressibility and lower C_S^{-1} values. Cholesterol is important for membranes because it helps fill packing defects. Moreover, when present at sufficiently high mole fractions, cholesterol enables rapid formation of highly-ordered (thicker), densely packed (less elastic), LO membrane regions. Thus, cholesterol can nearly completely eliminate packing defects in the sphingolipid/phospholipid lattice structure while enabling the rapid attainment of low elasticity packing states. We have observed similar behavior among sphingomyelins (26). Needham (47) also has noted

TABLE 1 Lateral packing properties of LacCers, GalCers, and SMs at 30 mN/m in the absence and presence of cholesterol

	Without cholesterol			With cholesterol (equimolar)		
Lipids	Area (Å^2)	C_S^{-1} (mN/m)	Phase state	Area (Å^2)	C_S^{-1} (mN/m)	Phase state
8:0 LacCer	55.3	124	LE	40.9	350	LO
16:0 LacCer	40.9	309	C	40.7	881	LO
18:0 LacCer	40.4	349	C	40.8	886	LO
18:1 LacCer	51.3	118	LE	39.7	304	LO
24:0 LacCer	40.6	308	C	39.9	671	LO
24:1 LacCer	42.6	144	C	41.6	440	LO
16:0 GalCer	39.6	607	C	38.2	1047	LO
18:0 GalCer	39.9	655	C	38.6	963	LO
18:1 GalCer	54.4	155	LE	40.4	494	LO
24:0 GalCer	41.9	391	C	39.2	678	LO
24:1 GalCer	37.3	372	LE	39.5	472	LO
16:0 SM	47.2	190	M	39.7	929	LO
18:0 SM	45.5	274	C	40.0	941	LO
18:1 SM	57.8	129	LE	40.0	353	LO
24:0 SM	47.4	167	C	40.6	644	LO
24:1 SM	60.5	107	M	41.8	362	LO

LE is liquid expanded phase (chain disordered, fluid); C is condensed phase (chain ordered, gel); M indicates coexisting liquid and condensed phases; and LO is liquid ordered phase.

All determinations were carried out at 30 mN/m, which mimics the biomembrane environment (52). Values for SMs and GalCers are in agreement with those of Li et al. (26) and Ali et al. (50), respectively.

Standard deviations for the C_S^{-1} values are $\pm\sim5\%$.

similar responses for saturated chain phosphatidylcholines during micropipette aspiration studies of bilayer elasticity. Metabolic alteration of cholesterol concentration could provide mammalian cells with a mechanism for rapidly adjusting lateral elasticity in target membranes containing sphingolipids. Cholesterol is ideally structured for accomplishing this task. With its single hydroxyl group for a polar headgroup, the sterol molecule can also act like a spacer to relieve mobility constraints among neighboring LacCer headgroups. The planar, cholestane ring provides a flat, rigid, hydrophobic surface that is ~9 Å long and well suited for interacting with saturated hydrocarbon chains (66–69). Because the polar hydroxyl moiety keeps the cholestane ring close to the interface, transient *trans-gauche* isomers are reduced in chain regions within ~11 Å of the interface where changes in lateral elasticity are expected to exert particularly strong effects.

What is also clear from this study is that the concentration of cholesterol is critical for modulating the lateral elasticity of LacCer with long saturated acyl chains. Although slight or no decrease in lateral elasticity is observed at low cholesterol mole fractions, marked changes occur at sterol mole fractions of 0.3 or higher. Similar abrupt increases in C_S^{-1}, i.e., reductions in lateral elasticity, also occur in SMs and PCs containing saturated acyl chains near 0.3 mol fraction of cholesterol and are known to correlate with onset of liquid-ordered phase behavior. Introduction of *cis* unsaturation or substantial shortening of the saturated acyl chain of LacCer acts to buffer the abruptness and diminish the extent of the decrease induced by cholesterol. In these fundamental ways, the interactions between different LacCer species and cholesterol mirror responses that have been observed with other simple sphingolipids, such as GalCer and SM (24–27,50,70).

It is important to emphasize that the observed area ''expansion effect'' of cholesterol with the saturated acyl chain LacCers is relatively small and never exceeds ~2 Å^2 (Fig. 2). Nonetheless, the effect is reproducible, depends on both surface pressure and cholesterol content, and leads to increased C_S^{-1} values at high pressure and high cholesterol content. One explanation for this apparently contradictory finding is the following scenario: At no or low sterol content ($\leq$0.2 mol fraction cholesterol) and high pressures, LacCers with saturated acyl chains are chain-ordered and have small cross-sectional areas consistent with the lactosyl (disaccharide) headgroups orienting more perpendicular than parallel to the surface (36). When the cholesterol content increases sufficiently high for LO phase formation to occur, the intermolecular ''spacer effect'' of the cholesterol is expected to be enhanced by the dramatic increase in lipid lateral diffusion rates associated with LO phase (compared to gel phase). As a result, the lactosyl group can be expected to become less and less orientationally restricted, enhancing its ''umbrella effect'' over cholesterol and increasing the average spacing between LacCer molecules (as reflected by the slightly larger average cross-sectional areas). The increase in the content of the less elastic cholesterol keeps the LacCer hydrocarbon chains ordered, resulting in the monolayer having less lateral compressibility. Although speculative, the preceding scenario is generally consistent with current ideas involving LO phase formation while invoking a role for changes in average headgroup orientation for controlling subtle changes in average cross-sectional area.

It is noteworthy that, although LacCer and SM both achieve similar low lateral elasticities at high cholesterol mole fractions, the pathways for achieving these similar packing states appear to differ. In the absence of cholesterol, LacCers with long saturated acyl chains display relatively high thermotropic phase transition temperatures and high C_S^{-1} values compared to the respective chain-matched SMs, suggesting that the lactose headgroup interferes less with attainment of tight intermolecular packing than the phosphorylcholine headgroup of SM (36). Thus the data suggest that the lactose headgroup projects from the monolayer interface in a more perpendicular than parallel fashion, contrasting the situation for SM where the charged zwitterionic headgroup is more highly hydrated and bulkier. Consistent with this scenario is the high sensitivity displayed by LacCer with saturated acyl chains to low cholesterol concentrations where small positive deviations from additivity are evident. At high sterol concentrations, however, the differences in headgroup structure between LacCer and SM become dampened by virtue of cholesterol acting as an intermolecular spacer and leads to the convergence of the respective C_S^{-1} values (Fig. 8, Table 1). Such a spacer effect of cholesterol could bring about increased accessibility to the sugar headgroup of LacCer by approaching macromolecules while keeping the GSL firmly anchored within a low elasticity microdomain within the membrane surface.

Compared to LacCers and SMs, the interactions of GalCers with cholesterol are not modulated as strongly by the sphingolipid headgroup. Comparison of C_S^{-1} values for several LacCers, GalCers and SMs, in the absence and presence of equimolar cholesterol at 30 mN/m (Fig. 8, Table 1) show that, when the ceramide region is identical and cholesterol is absent, the C_S^{-1} values (GalCer > LacCer > SM) correlate with hydrated headgroup size/orientation. In the presence equimolar of cholesterol, the already high C_S^{-1} values of GalCer rise even higher. However, the increase in C_S^{-1}, i.e., decrease in lateral elasticity, in going from the pure state to a cholesterol-GalCer equimolar mixture is less than that observed with LacCer and SM, probably because of the lower hydration capacity and less bulky nature of the monosaccharide headgroup.

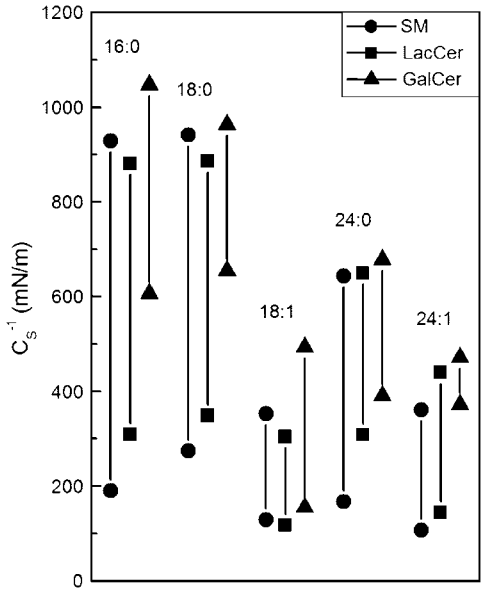

FIGURE 8 Comparison of surface compressional moduli (C_S^{-1}) of cholesterol mixed with different host sphingolipids. (●, SM, ■, LacCer, and ▲, GalCer). Lower C_S^{-1} values, no cholesterol; upper C_S^{-1} values, equimolar (50 mol %) cholesterol mixtures. All C_S^{-1} values determined at 30 mN/m surface pressure, which mimics the environment in biomembranes.

Implications

The studies here are the first to comprehensively characterize the lateral interactions between cholesterol and LacCers. The similarity in the lateral elasticity observed for LacCers and SMs at high cholesterol mole fractions is consistent with the reported localization of LacCer to the detergent resistant membrane fraction in biomembranes. More important is the accumulating body of work showing how increasing cholesterol content affects the lateral elasticity of phosphoglycerides and sphingolipids in monolayers and bilayers (e.g., 26,27,44,47,51,65,71). Such studies have helped develop recent ideas in which the resistance to lipid lateral compression/extension in bilayers has been identified as a key material property that strongly potentiates membrane thickness, i.e., hydrophobic mismatch, for driving the sorting and lateral localization of certain proteins (28–30). The manner in which increasing cholesterol content alters the lateral elasticity of LacCer further suggests that high cholesterol content could enable increased accessibility to the lactose headgroup by approaching macromolecules while keeping the glycolipid firmly anchored within the low elasticity membrane environment.

We gratefully acknowledge the support of United States Public Health Service grants HL49180 (H.L.B.) and GM45928 (R.E.B.), and the Hormel Foundation. Portions of this investigation were presented in preliminary form at the Biophysical Society Discussion: Probing Membrane Microdomains held in Asilomar, CA (Oct. 28–31, 2004) and at the 48th Annual Meeting of the Biophysical Society held in Baltimore, MD (Feb 14–18, 2004) and have been published in abstract form.

REFERENCES

1. Thompson, T. E., and T. W. Tillack. 1985. Organization of glycosphingolipids in bilayers and plasma membranes of mammalian cells. *Annu. Rev. Biophys. Chem.* 14:361–381.
2. Simons, K., and E. Ikonen. 1997. Functional rafts in cell membranes. *Nature*. 387:569–572.
3. Brown, D. A., and E. London. 1998. Functions of lipid rafts in biological membranes. *Annu. Rev. Cell Dev. Biol.* 14:111–136.
4. Mañes, S., G. del Real, and C. Martínez-A. 2003. Pathogens: raft hijackers. *Nature Rev. Immunol.* 3:557–568.

5. Edidin, M. 2003. The state of lipid rafts: from model membranes to cells. *Annu. Rev. Biophys. Biomol. Struct.* 32:257–283.
6. Mayor, S., and M. Rao. 2004. Rafts: scale-dependent, active lipid organization at the cell surface. *Traffic.* 5:231–240.
7. Mukherjee, M., and F. R. Maxfield. 2004. Membrane domains. *Annu. Rev. Cell Dev. Biol.* 20:839–866.
8. Simons, K., and W. L. C. Vaz. 2004. Model systems, lipid rafts, and cell membranes. *Annu. Rev. Biophys. Biomol. Struct.* 32:269–295.
9. Kusumi, A., and K. Suzki. 2005. Toward understanding the dynamics of membrane-raft-based molecular interactions. *Biochim. Biophys. Acta.* 1746:234–251.
10. Kusumi, A., C. Nakada, K. Ritchie, K. Murase, K. Suzuki, H. Murakoshi, R. S. Kasai, J. Kondo, and T. Fujiwara. 2005. Paradigm shift of the plasma membrane concept from the two-dimensional continuum fluid to the partitioned fluid: high speed single-molecule tracking of membrane molecules. *Annu. Rev. Biophys. Biomol. Struct.* 34:351–378.
11. Dietrich, C., Z. N. Volovyk, M. Levi, N. L. Thompson, and K. Jacobson. 2001. Partitioning of Thy-1, GM1, and cross-linked phospholipid analogs into lipid rafts reconstituted in supported model membrane monolayers. *Proc. Natl. Acad. Sci. USA.* 98:10642–10647.
12. Veatch, S. L., and S. L. Keller. 2002. Organization in lipid membranes containing cholesterol. *Phys. Rev. Lett.* 89:268101-1–268101-4.
13. De Almeida, P. F. M., A. Fedorov, and M. Prieto. 2003. Sphingomyelin/phosphatidylcholine/-cholesterol phase diagram: boundaries and composition of lipid rafts. *Biophys. J.* 85:2406–2416.
14. Stottrup, B. L., D. S. Stevens, and S. L. Keller. 2005. Miscibility of ternary mixtures of phospholipids and cholesterol in monolayers and application to bilayer systems. *Biophys. J.* 88:269–276.
15. Ipsen, J. H., G. Karlstrom, O. G. Mouritsen, H. Wennerstrom, and M. J. Zuckermann. 1987. Phase equilibria in the phosphatidylcholine-cholesterol system. *Biochim. Biophys. Acta.* 905:162–172.
16. Vist, M. R., and J. H. Davis. 1990. Phase equilibria of cholesterol/dipalmitoylphosphatidylcholine mixtures: ^{2}H nuclear magnetic resonance and differential scanning calorimetry. *Biochemistry.* 29:451–464.
17. Sankaram, M. B., and T. E. Thompson. 1990. Interactions of cholesterol with various glycerophospholipids and sphingomyelin. *Biochemistry.* 29:10670–10675.
18. Brown, R. E. 1998. Sphingolipid organization in biomembranes: what physical studies of model membranes reveal. *J. Cell Sci.* 111:1–9.
19. Silvius, J. R. 2003. Roles of cholesterol in lipid raft formation: lessons from lipid model membranes. *Biochim. Biophys. Acta.* 1610:174–183.
20. Bretscher, M. S., and S. Munro. 1993. Cholesterol and the Golgi apparatus. *Science.* 261:1280–1281.
21. Brown, D. A., and J. K. Rose. 1992. Sorting of GPI-anchored proteins to glycolipid-enriched membrane subdomains during transport to the apical cell surface. *Cell.* 68:533–544.
22. Ahmed, S. N., D. A. Brown, and E. London. 1997. On the origin of sphingolipid/cholesterol-rich detergent-insoluble cell membranes: physiologic concentrations of cholesterol and sphingolipids induce formation of a detergent-insoluble, liquid-ordered lipid phase in model membranes. *Biochemistry.* 36:10944–10953.
23. Parkin, E. T., A. J. Turner, and N. M. Hooper. 2001. Differential effects of glycosphingolipids on the detergent-insolubility of the glycosylphosphatidylinositol-anchored membrane dipeptidase. *Biochem. J.* 358:209–216.
24. Smaby, J. M., V. S. Kulkarni, M. Momsen, and R. E. Brown. 1996. The interfacial elastic packing interactions of galactosylceramides, sphingomyelins, and phosphatidylcholines. *Biophys. J.* 70:868–877.
25. Smaby, J. M., M. Momsen, V. S. Kulkarni, and R. E. Brown. 1996. Cholesterol-induced interfacial area condensations of galactosylceramides and sphingomyelins with identical acyl chains. *Biochemistry.* 35:5696–5704.
26. Li, X.-M., M. M. Momsen, J. M. Smaby, H. L. Brockman, and R. E. Brown. 2001. Cholesterol decreases the interfacial elasticity and detergent solubility of sphingomyelins. *Biochemistry.* 40:5954–5963.
27. Li, X.-M., M. M. Momsen, H. L. Brockman, and R. E. Brown. 2003. Sterol structure and sphingomyelin acyl chain length modulate lateral packing elasticity and detergent solubility in model membranes. *Biophys. J.* 85:3788–3801.
28. Lundbæk, J. A., O. S. Andersen, T. Werge, and C. Nielsen. 2003. Cholesterol-induced protein sorting: an analysis of energetic feasibility. *Biophys. J.* 84:2080–2089.
29. Allende, D. A., T. Vidal, and J. McIntosh. 2004. Jumping to rafts: gatekeeper role of bilayer elasticity. *Trends Biochem. Sci.* 29:325–330.
30. Allende, D., A. Vidal, S. A. Simon, and T. J. McIntosh. 2003. Bilayer interfacial properties modulate the binding of amphipathic peptides. *Chem. Phys. Lipids.* 122:65–76.
31. Sharma, D. K., J. C. Brown, Z. Cheng, E. L. Holicky, D. L. Marks, and R. E. Pagano. 2005. The glycosphingolipid, lactosylceramide, regulates β1-integrin clustering and endocytosis. *Cancer Res.* 65:8233–8241.
32. Puri, V., R. Watanabe, M. Dominguez, X. Sun, C. L. Wheatley, D. L. Marks, and R. E. Pagano. 1999. Cholesterol modulates membrane traffic along the endocytic pathway in sphingolipid-storage diseases. *Nat. Cell Biol.* 1:386–388.
33. Hakomori, S. 2003. Structure, organization, and function of glycosphingolipids in membrane. *Curr. Opin. Hematol.* 10:16–24.
34. Bektas, M., and S. Spiegel. 2004. Glycosphingolipids and cell death. *Glycoconj. J.* 20:39–47.
35. Degroote, S., J. Wolthoorn, and G. van Meer. 2004. The cell biology of glycosphingolipids. *Semin. Cell Dev. Biol.* 15:375–387.
36. Li, X.-M., M. M. Momsen, H. L. Brockman, and R. E. Brown. 2002. Lactosylceramide: effect of acyl chain structure on phase behavior and molecular packing. *Biophys. J.* 83:1535–1546.
37. Yu, Z., T. L. Calvert, and D. Leckband. 1997. Molecular forces between membranes displaying neutral glycosphingolipids: Evidence for carbohydrate attraction. *Biochemistry.* 37:1540–1550.
38. Momsen, W. E., J. M. Smaby, and H. L. Brockman. 1990. The suitability of nichrome for measurement of gas-liquid interfacial tension by the Wilhelmy method. *J. Colloid Interface Sci.* 135:547–552.
39. Smaby, J. M., and H. L. Brockman. 1991. A simple method for estimating surfactant impurities in solvents and subphases used for monolayer studies. *Chem. Phys. Lipids.* 58:249–252.
40. Kaganer, V. M., H. Möhwald, and P. Dutta. 1999. Structure and phase transitions in Langmuir monolayers. *Rev. Mod. Phys.* 71:779–819.
41. Ali, S., J. M. Smaby, M. M. Momsen, H. L. Brockman, and R. E. Brown. 1998. Acyl chain-length asymmetry alters the interfacial elastic interactions of phosphatidylcholines. *Biophys. J.* 74:338–348.
42. Li, X.-M., J. M. Smaby, M. M. Momsen, H. L. Brockman, and R. E. Brown. 2000. Sphingomyelin interfacial behavior: the impact of changing acyl chain composition. *Biophys. J.* 78:1921–1931.
43. Evans, E., and D. Needham. 1987. Physical properties of surfactant bilayer membranes: thermal transitions, elasticity, rigidity, cohesion, and colloidal interactions. *J. Phys. Chem.* 91:4219–4228.
44. Needham, D., and R. S. Nunn. 1990. Elastic deformation and failure of lipid bilayer membranes containing cholesterol. *Biophys. J.* 58:997–1009.
45. Davies, J. T., and E. K. Rideal. 1963. Interfacial Phenomena, 2nd ed. Academic Press, New York.
46. Merkel, R., and E. Sackmann. 1994. Nonstationary dynamics of excimer formation in two-dimensional fluids. *J. Phys. Chem.* 98:4428–4442.
47. Needham, D. 1995. Cohesion and permeability of lipid bilayer vesicles. *In* Permeability and Stability of Lipid Bilayers. E. A. Disalvo and S. A. Simon, editors. CRC Press, Boca Raton, FL. 49–76.
48. Behroozi, F. 1996. Theory of elasticity in two dimensions and its application to Langmuir-Blodgett films. *Langmuir.* 12:2289–2291.
49. Li, X.-M., M. Ramakrishnan, H. L. Brockman, R. E. Brown, and M. J. Swamy. 2002. *N*-Myristoylated phosphatidylethanolamine: interfacial behavior and interaction with cholesterol. *Langmuir.* 18:231–238.

50. Ali, S., J. M. Smaby, H. L. Brockman, and R. E. Brown. 1994. Cholesterol's interfacial interactions with galactosylceramides. *Biochemistry*. 33:2900–2906.

51. Smaby, J. M., M. Momsen, H. L. Brockman, and R. E. Brown. 1997. Phosphatidylcholine acyl unsaturation modulates the decrease in interfacial elasticity induced by cholesterol. *Biophys. J*. 73:1492–1505.

52. Marsh, D. 1996. Lateral pressure in membranes. *Biochim. Biophys. Acta*. 1286:183–223.

53. Cantor, R. S. 1999. Lipid composition and the lateral pressure profile in bilayers. *Biophys. J*. 76:2625–2639.

54. Maggio, B., D. C. Carrer, M. L. Fanani, R. G. Oliveira, and C. M. Rosetti. 2004. Interfacial behavior of glycosphingolipids and chemically related sphingolipids. *Curr. Opin. Colloid Interface Sci*. 8:448–458.

55. Vaknin, D., M. S. Kelley, and B. M. Ocko. 2001. Sphingomyelin at the air-water interface. *J. Chem. Phys*. 115:7697–7704.

56. Chatterjee, S. 1998. Sphingolipids in atherosclerosis and vascular biology. *Arterioscler. Thromb. Vasc. Biol*. 18:1523–1533.

57. Iwamoto, T., S. Fukumoto, K. Kanaoka, E. Sakai, M. Shibata, E. Fukumoto, J. Inokuchi, K. Takamiya, K. Furukawa, K. Furukawa, Y. Kato, and A. Mizuno. 2001. Lactosylceramide is essential for the osteoclastogenesis mediated by macrophage-colony-stimulating factor and receptor activator of nuclear factor-κB ligand. *J. Biol. Chem*. 49:46031–46038.

58. Gong, N., H. Wei, S. H. Chowdhury, and S. Chatterjee. 2004. Lactosylceramide recruits PCKα/ε and phospholipase A_2 to stimulate PECAM-1 expression in human monocytes and adhesion to endothelial cells. *Proc. Natl. Acad. Sci. USA*. 101:6490–6495.

59. Möhwald, H. 1995. Phospholipid monolayers. *In* Handbook of Biological Physics, Vol. 1. R. Liposky and E. Sackmann, editors. Elsevier Science, Amsterdam. 161–211.

60. Mombelli, E., R. Morris, W. Taylor, and F. Fraternali. 2003. Hydrogen-bonding propensities of sphingomyelin in solution and in a bilayer assembly: A molecular dynamics study. *Biophys. J*. 84:1507–1517.

61. Chiu, S. W., S. Vasudevan, E. Jakobsson, R. J. Mashl, and H. L. Scott. 2003. Structure of sphingomyelin bilayers: A simulation study. *Biophys. J*. 85:3624–3635.

62. Niemelä, P., M. T. Hyvönen, and I. Vattulainen. 2004. Structure and dynamics of sphingomyelin bilayer: Insight gained through systematic comparison to phosphatidylcholine. *Biophys. J*. 87:2976–2989.

63. Niemelä, P. S., M. T. Hyvönen, and I. Vattulainen. 2006. Influence of chain length and unsaturation on sphingomyelin bilayers. *Biophys. J*. 90:851–863.

64. Slotte, J. P., A.-L. Ostman, E. R. Kumar, and R. Bittman. 1993. Cholesterol interacts with lactosyl and maltosyl cerebrosides but not with glucoysl or galactosyl cerebrosides in mixed monolayers. *Biochemistry*. 32:7886–7892.

65. Kulkarni, V. S., and R. E. Brown. 1998. Thermotropic behavior of galactosylceramides with *cis*-monoenoic fatty acyl chains. *Biochim. Biophys. Acta*. 1372:347–358.

66. Hubbell, W. L., and H. M. McConnell. 1971. Molecular motion in spin-labeled phospholipids and membranes. *J. Am. Chem. Soc*. 93:314–326.

67. Rothman, J. E., and D. M. Engelman. 1972. Molecular mechanism for the interaction of phospholipid with cholesterol. *Nature (London). New Biol*. 237:42–44.

68. Davies, M. A., H. F. Schuster, J. W. Brauner, and R. Mendelsohn. 1990. Effects of cholesterol on conformational disorder in dipalmitoylphosphatidylcholine bilayers. A quantitative IR study of the depth dependence. *Biochemistry*. 29:4368–4373.

69. Morrow, M. R., D. Singh, D. Lu, and C. W. Grant. 1995. Glycosphingolipid fatty acid arrangement in phospholipid bilayers: cholesterol effects. *Biophys. J*. 68:179–186.

70. Smaby, J. M., H. L. Brockman, and R. E. Brown. 1994. Cholesterol's interfacial interactions with sphingomyelins and phosphatidylcholines: Hydrocarbon chain structure determines the magnitude of condensation. *Biochemistry*. 33:9135–9142.

71. Henriksen, J., A. C. Rowat, E. Brief, Y. W. Hsueh, J. L. Thewalt, M. J. Zuckermann, and J. H. Ipsen. 2006. Universal behavior of membranes with sterols. *Biophys. J*. 90:1639–1649.

72. Ruocco, M. J., D. J. Siminovitch, J. R. Long, S. K. Das Gupta, and R. G. Griffin. 1996. ^{2}H and ^{13}C nuclear magnetic resonance study of N-palmitoylgalactosylsphingosine (cerebroside)/cholesterol bilayers. *Biophys. J*. 71:1776–1788.